Functional dependence and quasiperiodicity in the spatiotemporal dynamics of yttrium iron garnet films

C. L. Goodridge, F. J. Rachford, L. M. Pecora, and T. L. Carroll
Code 6345, Naval Research Laboratory, Washington, DC 20375
(Received 12 September 2000; published 15 June 2001)

When thin films of yttrium iron garnet (YIG) are placed in a magnetic field and driven at microwave (rf) frequencies, nonlinear interactions within the material cause the normal microwave spin precession to be modulated at lower frequencies. We measure these lower frequency (kHz) signals at two spatially separated locations on the YIG film and use linear and nonlinear analysis to study the functional dependence of the spin dynamics at one location on the spin dynamics at the other location. We see dynamical states where nonlinear analysis can detect a functional dependence that the linear analysis fails to reveal.

DOI: 10.1103/PhysRevE.64.016210 PACS number(s): 05.45.Tp, 75.30.Ds

I. INTRODUCTION

The tools and techniques of nonlinear dynamics have gained wider utility with new applications occurring in fields from medicine to computer networks to condensed matter physics. Recent advances in nonlinear analysis techniques also allow researchers to gain new insight into previously studied systems. Yttrium iron garnet (YIG) is a technologically useful ferrimagnetic material with applications in devices such as microwave limiters, resonators, and filters [1]. Although the nonlinear properties of the dynamics of YIG have been studied and exploited for over fifty years, a complete understanding of the physics of this system has not been available [2]. Nonetheless, the nonlinear dynamics of chaotic low frequency oscillations in the ferromagnetic resonances of YIG films have been examined in detail by several groups [3–11].

When single crystal YIG films are placed in a saturating dc magnetic field, the electron spins align and precess around the direction of the dc field until damped out. An rf magnetic field at the precession frequency [12] applied perpendicular to the dc field will counteract the damping and maintain the precession [13–16] (Fig. 1). Since the spins are coupled, modulations in the phase of the individual spins produce spin waves traveling across the film surface. Standing surface waves corresponding to the modes of the film result when the spin waves are reflected at the film boundaries [17]. Initially these magnetostatic modes can be approximated as linear modes, but they are in fact coupled to a manifold of half-frequency modes of initially negligible amplitude. These modes can be derived from the Maxwell equations and the Landau-Lifshitz equation of motion for the magnetization

$$\frac{dM}{dt} = \gamma M H_T, \tag{1}$$

where γ is the gyromagnetic ratio, M is the magnetization, and H_T is the effective magnetic field. H_T is a function of the applied dc field, the microwave drive field, as well as dipole fields due to the magnetization of the sample. It is this term that makes the Landau-Lifshitz equation nonlinear. A damping term is often included as well. Above a threshold rf power (the Suhl instability) [2], the half-frequency modes gain power at the expense of the linear modes. Nonlinearities begin to dominate the dynamics as these half-frequency modes grow in amplitude, causing low frequency modulations of the spin precession amplitude at kHz frequencies. These periodic oscillations are called autooscillations and typically occur at powers just beyond the Suhl instability. As the applied rf power is increased, these oscillations may exhibit quasiperiodic and/or chaotic dynamics.

We detect spin precession in the YIG film by using probes consisting of small wire loops perpendicular to the plane of the film. The out-of-plane component of the magnetic precession produces a time-varying magnetic flux through the loop, which induces a varying voltage, which is the signal that we measure. Previous researchers have studied these dynamics in both spheres (which have an attractive symmetry which simplifies analysis and are readily available) and thin films of YIG. Chaotic transients and attractors as well as solitons have been described and analyzed [3–6]. Aspects such as control and synchronization of chaotic oscillations in YIG films have also been experimentally studied [9,10]. Recent experiments have investigated mode interactions in these films such as how the application of two driving frequencies affects the Suhl instability [7,8]. These earlier experiments concentrated on the global response of YIG samples and analyzed the temporal dynamics of the entire sample. Few aspects of the spatial dynamics of this system have been previously studied and characterized except in the linear regime and near the Suhl instability. In the experiments described here, we explore the local dynamics of YIG films experiencing global driving with the goal of characterizing the spatial dynamics across the film surface [18]. The magnetic resonance in a YIG film is monitored using a pair of probes placed at two spatially separated positions on the

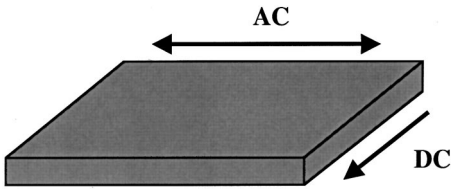

FIG. 1. The YIG film is subjected to perpendicular dc and rf magnetic fields to produce spin waves dynamics.

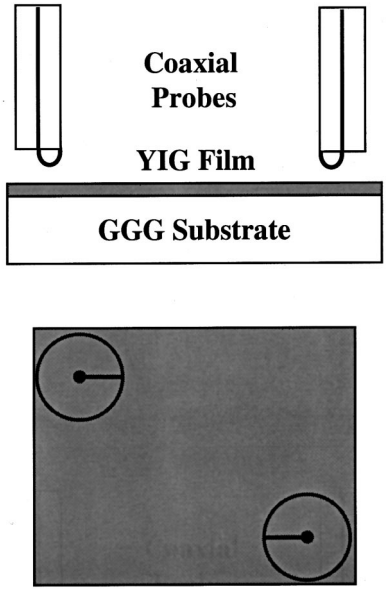

FIG. 2. Coaxial probes detect the magnetic moment of the YIG film at two positions. The probes are aligned as shown to maximize signal strength while minimizing interference between the probes and pickup from the excitation field.

film. Our measurements indicate that it is possible to create quasiperiodic states with two noncommensurate frequencies that vary in intensity at each probe.

II. EXPERIMENT

Our sample is a rectangular film cut from a single crystal of YIG grown by liquid-phase epitaxy on a gadolinium-gallium-garnet (GGG) substrate. The film has dimensions $0.85\times0.72\,\mathrm{cm}^2$ and is 37 μm thick. The spin wave modulations are detected by mounting two probes adjacent to the film surface. These probes are constructed by connecting the inner conductor of OS-80 coaxial cable to the outer conductor, forming a small pickup loop. The probes are aligned as shown in Fig. 2.

A diagram of the experimental system is shown in Fig. 3. The GHz spin wave signals were amplified using low noise Miteq AFS3 microwave amplifiers (providing 35–36 dBm amplification). The kHz modulations are detected using Schottky diode detectors. The signals then are amplified using a Stanford Research Systems 560 analog amplifier and an EG&G PARC 113 analog amplifier and digitized using a National Instruments I/O board. The dc field was controlled to within 0.01 Oe by a varian fieldial regulator and measured with a Lakeshore 450 Gaussmeter. A HP 8341 Synthesized Sweeper supplied the rf excitation power.

The detected auto-oscillations varied in frequency from 2 to 12 kHz. Setting three parameters specified each individual state: the dc magnetic field, the resonant rf field frequency, and the rf field power. Table I summarizes the experimental parameters. The resonance spectrum of this film is shown in Fig. 4. We excite the spin waves at 2.9747 GHz, which corresponds to the (5,0) surface mode of the film. Data were gathered by fixing the dc intensity and the rf frequency and

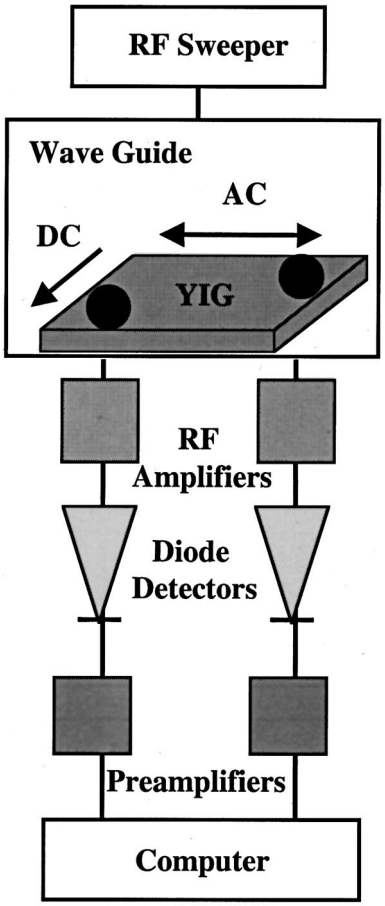

FIG. 3. The YIG film and probes are mounted at the bottom of a wave guide and an rf field provided by an rf synthesized sweeper excites spin waves. The resulting voltage signals are processed by a series of amplifiers and diode detectors.

then varying the rf power and consist of two simultaneously sampled time series, corresponding to the voltage signals from the individual probes. An initial rf power intensity that produced a periodic signal from both probes was selected as the starting point and then the power was increased in small increments.

III. RESULTS AND ANALYSIS

The goal of our analysis is to investigate the functional dependence between the two time series to better describe the spatial aspects of the film dynamics using both linear and

TABLE I. Experimental parameters. The rf field frequency, rf field power, and dc field strength determine the states studied.

Parameter	Range
rf Frequencies	2.9747 Ghz
rf (Source) Power	3–10 dBm
dc Field	449.9 Oe
Number of samples	65536 Points
Sampling rate	625000 Samples/s

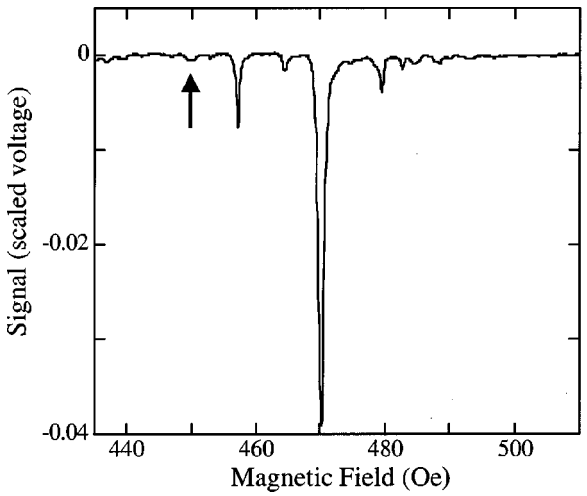

FIG. 4. The resonant spectrum of a $0.85\times0.72\,\mathrm{cm}^2$ YIG film of thickness 37 μm subjected to a 2.9747 GHz rf field. The arrow points to the mode we excite in these experiments, which is the (5,0) surface mode.

nonlinear techniques. We determine the power spectra and use these results to find the strongest frequencies present in each time series. We used the cross-correlation C_r to investigate the linear relationship between the two signals as well as two nonlinear statistics Θ_{c0} and Θ_{c0} beyond linear, developed by the authors. These statistics allow for the characterization of several nonlinear properties of the relationship between the two time series [19–21]. Both of these nonlinear statistics quantify the functional dependence from the first time series to the second time series. A brief description of this technique is outlined in the appendix and a complete description can be found in Goodridge *et al.* [22].

The spin wave states produced at the parameters listed in Table I exhibited two transitions as the rf power is increased. Throughout the entire power sweep, the detected signals were predominately periodic in nature with frequencies between 2 and 12 kHz. However, there is a region of rf powers, between 5.4 and 7.4 dBm, where the dynamics become quasiperiodic. The two frequencies present in each of these states are noncommensurate. The linear functional dependence and the cross-correlation between these time series decreases in this range but there is still some functional dependence present. Above 7.4 dBm, the states become periodic again with more broadband dynamics present at higher powers.

Three examples of the time series measured in these experiments are shown in Fig. 5. The individual time series measured at 4.4 and 7.6 dBm are periodic with similar power spectra. This is contrasted with the data from the state produced at 6.0 dBm, where the time series are quasiperiodic. There are two strong frequencies present in this state, 3.3 and 11.1 kHz. In the time series measured at probe 1, the 11.1 peak is much more intense than the 3.3 kHz peak. At probe 2, the 3.3 kHz signal is dominant. This behavior occurs in nearly all of the states between 5.4–7.4 dBm. This is shown in Fig. 6, where the ratios of the spectral powers of the noncommensurate frequencies are plotted. The values are calculated by first measuring the power level of both the low and

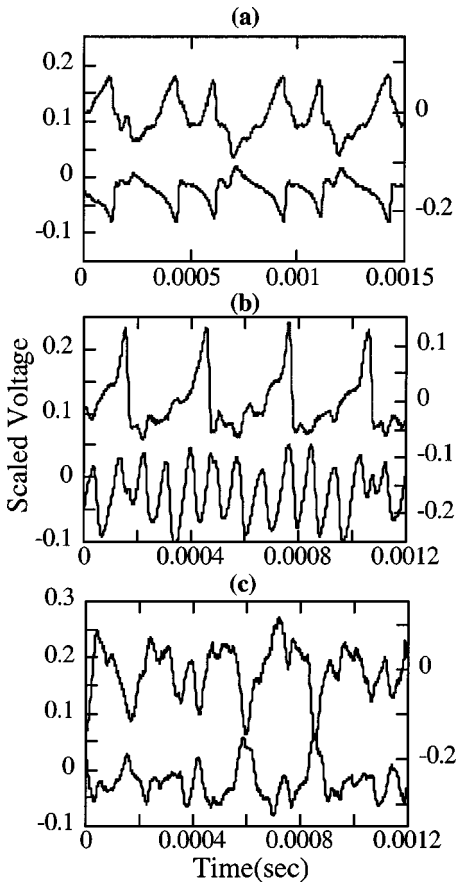

FIG. 5. Three plots of the time series produced in these experiments. The top trace corresponds to the signal from probe 2; the bottom trace corresponds to the signal from probe 1. The rf power for each state is (a) 4.4 dBm, (b) 6.0 dBm, and (c) 9.2 dBm. States (a) and (c) exhibit identical dominant frequencies, 2.2 and 4.9 kHz, respectively. State (b) produced quasiperiodic time series with two noncommensurate frequencies, 3.3 and 11.1 kHz, which dominate the dynamics at probe 2 and probe 1, respectively. Scaled voltage is plotted against acquisition time and the traces are offset to facilitate viewing.

high frequencies in the power spectrum from each time series. This gives us two values for each time series, the power level of the low frequency and that of the higher frequency. The ratio is then calculated by dividing the power level of the low frequency by that of the higher frequency. In most of these time series, the power at one frequency is several orders of magnitude larger than the power at the other frequency, indicating that one frequency plays a stronger roll in the dynamics than does the other. In this power range, probe 1 consistently sees stronger signals from the higher frequencies; the reverse is true for probe 2.

Several other states deserve additional discussion. In general, spin wave states in YIG will evolve from periodic to chaotic dynamics as the applied rf power is increased. However, under certain parametric conditions (dc field strength, rf frequency, and rf amplitude), periodic and chaotic windows can be observed as power is increased. The state at 3.4 dBm where neither probe detected periodic or quasiperiodic behavior is an example of such a window. Both time series

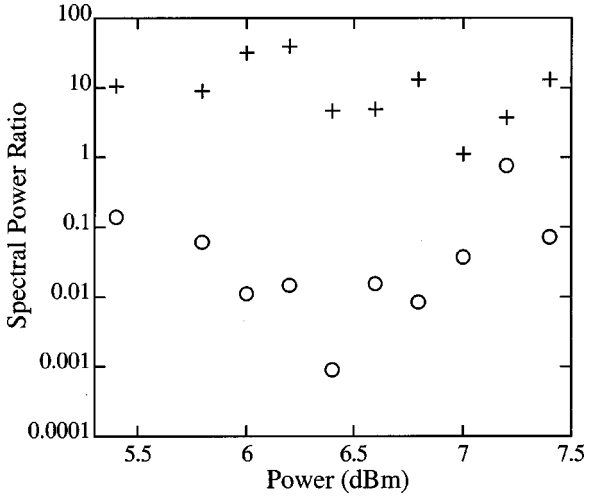

FIG. 6. A plot of the ratios of the spectral powers for the two strongest frequencies in each of the quasiperiodic states. These values are determined by dividing the measured spectral power of the lower of the two noncommensurate frequencies by the spectral power of the higher frequency. The symbols + and *O* correspond to the ratios from time series 1 and time series 2, respectively.

produced broadband power spectra, possibly indicating high-dimensional chaotic behavior. More interesting are the states produced at 5.6 dBm and at 9.6 and 9.8 dBm. Both time series measured at 5.6 dBm are periodic, revealing a periodic window inside the region of quasiperiodicity. Finally at both 9.6 and 9.8 dBm, one probe is detecting a periodic signal while the other is detecting a broadband or chaotic signal. Concurrent chaotic and periodic regions may be present in these states, perhaps similar to phenomena observed in Faraday waves [23].

The dynamics of this system require us to use statistics other than the cross-correlation to adequately characterize the functional dependence between film positions. Figure 7 shows three statistics (cross correlation, function statistic, and function statistic beyond linear) for the states produced in this power sweep. The cross correlation between the signals from the two probes is initially high and then drops off in the quasiperiodic region and then increases when the states become periodic again. This result implies that there is only weak *linear* functional dependence in the 5.4–7.4 dBm range. Note the high value for the periodic state at 5.6 dBm. The function statistic is a nonlinear measure of the functional dependence from time series 1 to time series 2. The high values for this statistic indicate that there is functional dependence even in the region of low cross-correlation values. The high values for the function statistic beyond linear (also a measure of the functional dependence from time series 1 to time series 2) indicate that some nonlinear functional dependence exists for all of these states, even those with little or no linear correlation. These high values also indicate that nonlinearities dominate the relationship between the time series in the 5.4–7.4 dBm range.

In order to verify that this phenomenon is due to the dynamics of the system and not due to an increase in the stochastic noise level, we plot values for three different noise measures in Fig. 8. σ is a meaningful length scale for a given

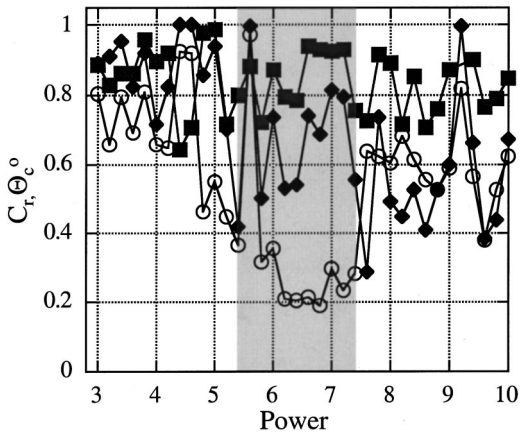

FIG. 7. A plot of the maximum cross-correlation *O*, the function statistic ◆, and the function statistic beyond linear ■ for the power sweep performed at 2.9747 GHz and 449.9 Oe. The quasiperiodic region is indicated by the shading. Periodic states with matching dominant frequencies are much more strongly linearly correlated than the quasiperiodic power states but high values for the function statistic beyond linear indicate that there is a nonlinear relationship present across the entire power range. The three statistics are unitless and range from 0 (no correlation) to 1 (total correlation).

time series (determined during the calculation of the nonlinear function statistic), η is the variance of the residues from a least squares linear fit model between the time series, and γ is a measure of the stochastic noise and is determined using the gamma test [24]. The values for the γ statistic remain roughly the same size over the range of powers indicating that the noise levels in the different states are roughly the same relative to the signal strength. The differences between the three correlation statistics are not caused by changing

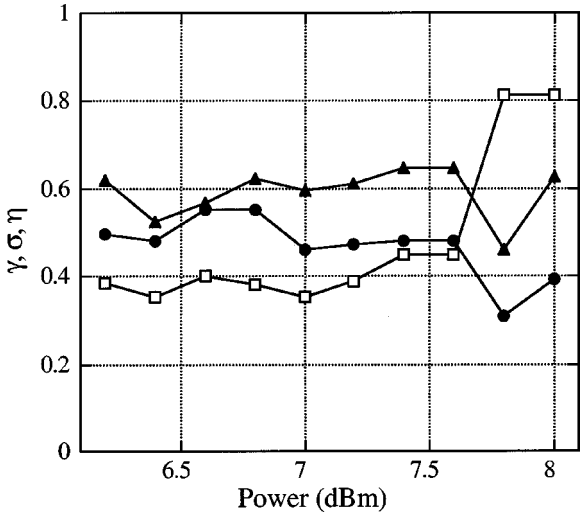

FIG. 8. Plots of two different noise levels: γ (a measure of the stochastic noise level of the time series data) ▲, σ (found during the calculation of functional significance) □, and η (the variance of the residues from a least squares linear model) ●. The relative closeness of the three statistics demonstrates that the observed variations in the correlation statistics are not due to an increase in the stochastic noise level experienced by the system.

noise levels and the observed changes in periodicity are due to the dynamics of the system and not due to an increase in the stochastic noise level experienced by the system.

IV. CONCLUSIONS

We have observed and described a set of quasiperiodic spin wave states produced in a YIG film that exhibits spatial variation of the observed frequency spectra. These states have minimal linear functional dependence but even as these auto-oscillations lose their periodic structure and linear correlation, there is still some nonlinear functional dependence, as illustrated by the high values for the nonlinear function statistics. Our results indicate that there is some relationship between the magnetic dynamics of surface wave modes sampled at spatially separated positions on the film surface and that this relationship is predominately nonlinear in character. The existence of functional dependence between the time series matches our expectations that the time series data should be related because the data are measured at two positions on a single spatially extended system. A more thorough investigation of these quasiperiodic states could be accomplished by using additional probes placed across the entire film surface. This would allow for investigation of the spatial dynamics of the entire film and perhaps for the determination of any correlation length scales that may exist.

ACKNOWLEDGMENTS

The authors wish to thank D. King, W. Lechter, and J. Valenzi for technical assistance. C. L. Goodridge acknowledges support from an Office of Naval Research/American Society.

APPENDIX: NONLINEAR ANALYSIS

This analysis calculates a pair of statistics that measure the degree of functional dependence between two simultaneously sampled time series and builds on previous work that described techniques to quantify continuity between functions relating time series [20–22]. High values for these statistics indicate that strong functional dependence exists between the time series. One statistic is a measure of the functional dependence between the time series; the other is a measure of the strength of the nonlinear component of the relationship between the time series.

Given two simultaneous time series $\{g_1,g_2,g_3,\ldots\}$ and $\{h_1,h_2,h_3,\ldots\}$, we construct vectors $\mathbf{x}_i$ and $\mathbf{y}_i$ and attractors $\mathbf{X}$ (the source) and $\mathbf{Y}$ (the target), such that $\mathbf{x}_i=(h_i,h_{i+\tau},\ldots,h_{i+\tau*(d-1)})\in\mathbf{X}$ and $\mathbf{y}_i=(g_i,g_{i+\tau},\ldots,g_{i+\tau*(d-1)})\in\mathbf{Y}$ by time delay embedding with dimension d and time delay τ. $\mathbf{x}$ and $\mathbf{y}$ are defined as corresponding points if the indices of the first coordinates are equal (i.e., simultaneous in time). Any set of embedding parameters (d,τ) that adequately characterizes the system dynamics will produce useful results and we use $d=5$ and $\tau=10$ here. We assume that there is a continuous function $\mathbf{F}$ relating the two time series such that $\mathbf{y}_i=\mathbf{F}(\mathbf{x}_i)$. Since $\mathbf{F}$ may be difficult to determine explicitly, we instead calculate a function statistic Θ_{c^0} that quantifies the strength of $\mathbf{F}$ and therefore describes how accurately we can make predictions between the two time series.

In order to calculate the function statistic, we divide the source attractor into clusters of points and calculate a value for the function statistic Θ_{c^0} for each cluster. This value is a measure of the local predictability between points in that cluster and the corresponding points on the other attractor. This calculation is then repeated for a number of other clusters and the resulting values are averaged to find an attractor wide value for the function statistic. These values are calculated using the significance of the variance for the points in each cluster. We calculate the variances and quantify the strength of the predictability using the significance of the variance with reference length scale σ. The significance of the variance is defined as the probability that the actual variance is larger than a given value, using σ^2 as the mean variance. We first determine a value for the length scale σ and then use that value to calculate the function statistic Θ_{c^0}. The probability distribution function for the variance is derived using the central limit theorem.

This analysis can be modified to test for nonlinearity in the functional relationship between two time series and produces a function statistic that is a measure of how much more accurate a nonlinear prediction is than a strictly linear prediction. The procedure is simple to implement. First, we fit the attractors to a linear model such as a least squares fit and determine the variance of the residues η from this model, then use this η for the scale σ in the significance calculation and follow the procedure outlined above. If there is a strong linear relationship, η and σ are on the same order and the values for the function statistic are low. If there are nonlinear components to the relationship between the time series, then $\eta>\sigma$ (implying that the error is high from a strictly linear model) and the values for the function statistic are high.

[1] B. Lax and K. J. Button, *Microwave Ferrites and Ferrimagnetics* (McGraw-Hill, New York, 1962).
[2] H. Suhl, J. Phys. Chem. Solids **1**, 209 (1957).
[3] T. L. Carroll, L. M. Pecora, and F. J. Rachford, Phys. Rev. Lett. **59**, 2891 (1987).
[4] T. L. Carroll, L. M. Pecora, and F. J. Rachford, Phys. Rev. B **38**, 2938 (1988).
[5] T. L. Carroll, L. M. Pecora, and F. J. Rachford, Phys. Rev. A **40**, 377 (1989).
[6] T. L. Carroll, L. M. Pecora, and F. J. Rachford, IEEE Trans. Magn. **27**, 5441 (1991).
[7] D. J. Mar *et al.*, J. Appl. Phys. **80**, 1878 (1996).
[8] D. J. Mar *et al.*, J. Appl. Phys. **81**, 5734 (1997).
[9] D. W. Peterman, M. Ye, and P. E. Wigen, Phys. Rev. Lett. **74**, 1740 (1995).
[10] M. Ye, D. W. Peterman, and P. E. Wigen, Phys. Lett. **203**, 23

(1995).
[11] G. Gibson and C. Jeffries, Phys. Rev. A **29**, 811 (1984).
[12] The resonant modes have frequencies set by both the applied dc field and the film geometry and occur at radio (GHz) frequencies.
[13] M. Chen and C. E. Patton, in *Nonlinear Phenomena and Chaos in Magnetic Materials* (World Scientific, Singapore, 1994).
[14] M. J. Hurben and C. E. Patton, J. Magn. Magn. Mater. **139**, 263 (1995).
[15] C. Patton, in *Magnetic Oxides*, edited by D. J. Craik (Wiley, London, 1975), p. 575.
[16] C. Patton, Phys. Lett. **103**, 251 (1984).
[17] R. W. Damon and J. R. Eshbach, J. Phys. Chem. Solids **19**, 308 (1961).
[18] C. Goodridge (unpublished).
[19] L. Pecora, T. Carroll, and J. Heagy, Phys. Rev. E **52**, 3420 (1995).
[20] D. T. Kaplan, Phys. Rev. D **73**, 38 (1994).
[21] S. Schiff *et al.*, Phys. Rev. E **54**, 6708 (1996).
[22] C. Goodridge *et al.* (unpublished).
[23] B. Gluckman, C. Arnold, and J. Gollub, Phys. Rev. E **51**, 1128 (1995).
[24] A. Stefansson and A. J. Jones, Neural Comput. Appl. **5**, 131 (1997).